

## QUASI LINEAR ALGORITHM FOR MODELLING SHORELINE CHANGE FROM AIRSAR/POLSAR POLARIZED DATA

Maged Marghany, Mazlan Hashim and Arthur P. Cracknell

Department of Remote Sensing

Faculty of Geoinformation Science and Engineering

Universiti Teknologi Malaysia

81310 UTM, Skudai, Johore Bahru, Malaysia

Email: [maged@fksg.utm.my](mailto:maged@fksg.utm.my),

[magedupm@hotmail.com](mailto:magedupm@hotmail.com),

[mazlan@fksg.utm.my](mailto:mazlan@fksg.utm.my),

[cracknellarthur@hotmail.com](mailto:cracknellarthur@hotmail.com)

### ABSTRACT

This paper presents a new approach for modeling shoreline change due to wave energy effects from remotely sensed data. The airborne AIRSAR and POLSAR data were employed to extract wave spectra information and integrate them with historical remotely sensed data such as aerial photography data to model the rate of change of the shoreline. A partial differential equation (PDF) of wave conversation model was applied to investigate the wave refraction patterns. The volume of sediment transport at several locations was estimated based on the wave refraction patterns. The shoreline change model developed was designed to cover a 14 km stretch of shoreline of Kuala Terengganu in peninsular Malaysia. The model utilized data from aerial photographs, AIRSAR, POLSAR and ERS-2 and in situ wave data.

The results showed that the shoreline change rate modeled from the quasi-linear wave spectra model has a significant relationship with one modeled from historical vector layers of aerial photography, AIRSAR and POLSAR data. With the quasi-linear model an error of  $\pm 0.18$  m/year in shoreline change rate determination was obtained with  $C_{vv}$  band. According to the above prospective, small polarized microwave sensor mounts on satellite platform might be provided similar out put results for shoreline change predictions. In fact, microwave spectra can be used with such tropical climate circumstances of cloud covers due to its longer wavelength and its polarization properties. As different polarization behaviour enable to study several coastal problems such as wave- current interaction, and wave-shoreline interaction.

**Keywords:** AIRSAR,POLSAR, quasi-linear, wave spectra, wave refraction, shoreline change.

### 1.INTRODUCTION

Synthetic Aperture Radar (SAR) has been recognized as a powerful tool for modeling ocean waves and forecasting over an area of 300 km x 300 km. Hence, the sediment transport could be modeled by the wave spectra information extracted from a SAR image. Currently, a number of investigations have been carried out on the assimilation of SAR wave mode data into wave forecasting models. This is because the SAR image spectrum has turned out to be far removed from the actual wave spectrum and rather complicated post-processing is necessary for extracting quantitative wave information In this regards, previous studies were carried out by Beal et al., (1983), Hasselmann and Hasselmann,

(1991), Vachon et al. (1994) and Forget and Brochel (1995) to develop an inversion algorithm to map SAR wave spectra into ocean wave spectra. Hasselmann and Hesselman (1991) introduced a non-linear algorithm which was developed by Vachon et al. (1995) to model the significant wave height based on the azimuth cut-off. Vachon et al. (1995) defined the azimuth cut-off as the degree to which the SAR image spectrum is constrained in the azimuth direction. The azimuth cut-off is affected by the wind and wave condition in a quasi-linear forward-mapping model (Vachon et al. 1997). Maged (2001) utilized the azimuth cut-off model which was developed by Vachon et al. (1995) to estimate the significant wave height. Based on the significant wave height information derived from two ERS-1 scenes, shoreline change rate has been modeled. In addition, Maged (2001) compared the shoreline change model based on the azimuth cut-off model and the shoreline observed by the Canny automatic detection algorithm. However, the accuracy of this study was very low due to the effect of velocity bunching.

The question can be raised as to how an integration of AIRSAR data with different sources of data such as historical ship wave observations, aerial photography and in situ wave measurements could be used to develop a new approach for the investigation of shoreline change with high accuracy and reduced error rate. The main objective of this study is to examine waves and wave effects on the Terengganu coastline using remote sensing data. The sub-objectives are: (1) to utilize AIRSAR data in the investigation of the wave spectral effect on the Terengganu coastline, (2) to model the physical properties of wave spectra refraction, (3) to model shoreline change based on the wave spectra model and (4) to identify erosion and sedimentation areas based on the wave energy input to the coastline.

## **2. METHODOLOGY**

### **2.1. Study Area**

The study area is located along the coast of Kuala Terengganu in the eastern part of Peninsular Malaysia. The area is approximately 14 km north of Kuala Terengganu coastline, located in the South China Sea between 5° 21' N to 5° 27' N and 103° 10' E to 103° 15' E. Sand materials make up the entire of the shoreline (Wong, 1981; Lokman et al., 1995; Maged, 2000). This area lies in an equatorial region dominated by two seasonal monsoons. The southwest monsoon lasts from May to September while the northeast monsoon lasts from November to March. The monsoon winds affect the direction and magnitude of the waves. Strong waves are prevalent during the northeast monsoon when the prevailing wave direction is from the north (November to March), while during the southwest monsoon (May to September), the wave directions are propagating from the south (Rosnan, 1987). According to Wong (1981) the maximum wave height during the northeast monsoon season is 4 m. The minimum wave height is found during the southwest monsoon which is less than 1 m.

### **2.2 Data Acquired**

#### **2.2.1 In Situ Wave Collection**

The sea wave truth data was collected by wave rider buoy from the Malaysian Meteorological service between latitudes of 5° 18' N and 5° 26' N and longitude of 103° 32' E 103° 40' E on 6 December 1996 and 19 September 2000 (during that time, the airborne AIRSAR was flown over the study area). The in situ observation data included

wave height and wave direction which were used for wave spectra modulation with AIRSAR data.

The wind data were collected at the Meteorological Station at Sultan Mahmed Airport, Kuala Terengganu, at latitudes of  $5^{\circ} 23' N$  and longitude of  $103^{\circ} 06'$  and obtained by the Malaysia Meteorological Service in Kuala Terengganu (Figure 1). Wind speed data were used to determine the azimuth cut-off modeled in AIRSAR data. The azimuth cut-off was used to model the significant wave height from AIRSAR SAR data which was based on the least squares fit algorithm. A least squares algorithm was applied between azimuth cut-off wavelength and geophysical parameters such as significant wave height (Vachon et al. 1994).

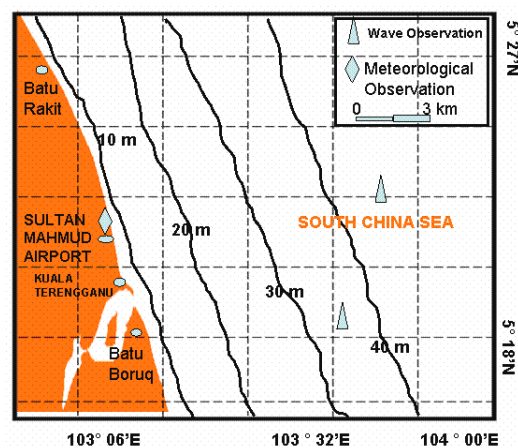


**Figure 1. Locations of in situ data collections**

### 2.2.2 AIRSAR and POLSAR Data

The Jet Propulsion Laboratory (JPL) airborne Airborne Synthetic Aperture Radar (AIRSAR) data were acquired on 6 December 1996 and 19 September 2000 from the coastline of Kuala Terengganu, Malaysia between  $103^{\circ} 5'E$  to  $103^{\circ} 9'E$  and  $5^{\circ} 20'N$  to  $5^{\circ} 27'N$ . AIRSAR is a NASA/JPL multi-frequency instrument package aboard a DC-8 aircraft and operated by NASA's Ames Research Center at Moffett Field. AIRSAR flies at 8 km over the average terrain height at a velocity of  $215 \text{ m s}^{-1}$ . The system is designed to be flown on small and large aircraft. The system requires a scanner port (18 cm x 36 cm) on the aircraft underside. JPL's airborne synthetic aperture radar (AIRSAR) is a unique system, comprising three radars at HH-, VV-, HV- and VH-polarized signals from 5m x 5m pixels recorded for three wavelengths: C band (5 cm), L band (24 cm) and P band (68 cm) (Zebker 1992). AIRSAR data collections are involved; fully polarimetric data (POLSAR) can be collected at all three frequencies, while cross-track interferometric data (TOPSAR) and along-track interferometric (ATI) data can be collected at C- and L-bands. This study utilizes the  $C_{VV}$  band of AIRSAR and POLSAR images for modeling shoreline change because of the widely known facts of good interaction of VV polarization to oceanographic physical elements such as ocean waves (Vachon et al. 1994).

The shoreline change model, see Figure 2, utilized wave spectra detection and shoreline change based on the volume rate change of sediment transport.

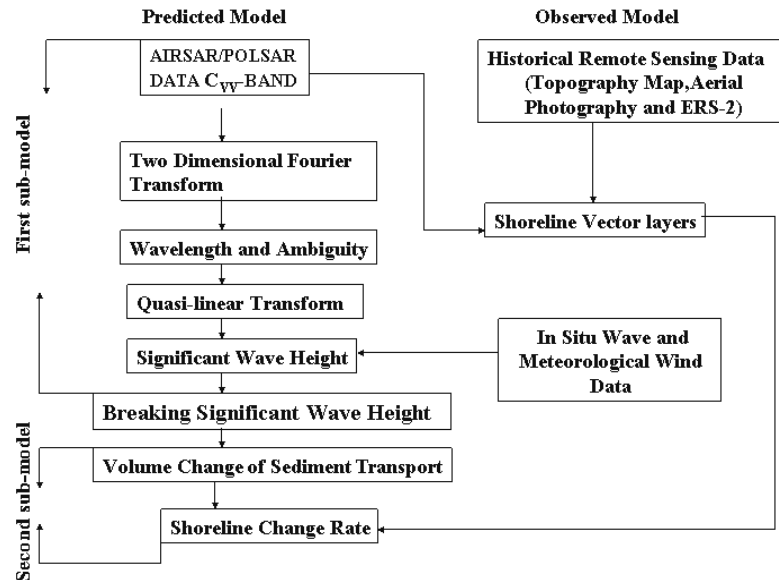


**Figure 2. Block diagram of shoreline change model from AIRSAR data**

### 2.3 AIRSAR and POLSAR Wave Spectra

In this study, a single AIRSAR and POLSAR images frame comprising of 315 x 315 image pixels was extracted from AIRSAR and POLSAR C<sub>vv</sub>-band. Each pixel represents a 10 m x 10 m area. The entire image frame of AIRSAR/POLSAR data corresponded to a 2 km x 2 km patch on the ocean surface. AIRSAR and POLSAR images are a two dimensional sampling of the ocean wave field and thus a two-dimensional (2-D) Fourier transfer has to be utilized (Populus et al., 1991 and Cornet et al., (1993). When the Fourier transfer was selected, the output domain is the two-dimensional frequency spectrum of the input image (Tukey, 1961).

#### 2.3.1 Quasi-linear Transform

To map observed SAR spectra into the ocean wave spectra, a quasi-linear model was applied. The simplified quasi-linear theory is explained below: according to the Gaussian linear theory, the relation between ocean wave spectra  $S(\mathbf{K}, \phi)$  and AIRSAR image spectra  $S_o(\mathbf{K})$  could be described by tilt and hydrodynamic modulation (real aperture radar (RAR) modulation). The tilt modulation is linear to the local surface slope in the range direction i.e. in the plane of radar illumination. The tilt modulation in general is a function of wind stress and wind direction for ocean waves and AIRSAR/POLSAR polarization. According to Vachon et al., (1994) the tilt modulation is the largest for HH polarization. Alpers et al., (1981) and Alpers and Bruning (1986) reported that hydrodynamic interaction between the scattering waves (ripples) and longer gravity

waves produced a concentration of the scatterer on the up wind face of the swell. Following Vachon et al., (1995) AIRSAR image spectra can map into ocean wave spectra under the assumption of the quasi-linear modulation transfer function  $S_Q(K)$  which is given by

$$S_Q(K) = R(K)H(k_i; K_c) \left[ \frac{S(K, \phi)}{2} |T_{lin}(k_{ij})|^2 + \frac{S(-K, \phi)}{2} |T_{lin}(-k_{ij})|^2 \right] \quad (1)$$

where  $H(k_i; K_c)$  is an azimuth cut-off function that depends upon azimuth wave number and range wave number  $k_{ij}$ , the cut-off azimuth wave number  $K_c$  and  $R(K)$  is the AIRSAR point spread function. The AIRSAR/POLSAR point spread function is a function of the azimuth and the range resolutions (Vachon et al., 1997). According to Vachon et al., (1994)  $T_{lin}$  is a linear modulation transfer function which is composed of the RAR (the tilt modulation and hydrodynamic modulation), and the velocity bunching modulation. The RAR modulation transfer function (RAR MTF) is the coherent sum of the transfer function associated with each of these terms.

#### 2.4. Significant Wave Height Model

In order to estimate the significant wave height from the quasi-linear transform, we adapted the algorithm that was given by Vachon et al., (1994) to be appropriate for the geophysical conditions of tropical coastal waters:

$$\lambda_c = \beta \left( \int_{H_{s0}}^{H_{sn}} \sqrt{H_s} dH_s + \int_{U_0}^{U_n} \sqrt{U} dU \right) \quad (2)$$

where  $\lambda_c$  is cut-off azimuth wavelength,  $H_s$  and  $U$  are the in situ data of significant wave height and wind speed along the coastal waters of Kuala Terengganu, Malaysia. The measured wind speed was estimated at 10m height above the sea surface. The changes of significant wave height and wind speed along the azimuth direction are replaced by  $dH_s$  and  $dU$ , respectively. The subscript zero refers to the average in situ wave data collected before flight pass over by two hours while the subscripts  $n$  refers to the average of in situ wave data during flight pass over the study area.  $\beta$  is an empirical value which results of  $R/V$  multiplied by the intercept of azimuth cut-off ( $c$ ) when the significant wave height and the wind speed equal zero. A least squares fit was used to find the correlation coefficient between cut-off wavelength and the one calculated directly from the AIRSAR/POLSAR spectra image by equation (2). Then, the following equation was adopted by Maged (2003) to estimate the significant wave height ( $H_{sT}$ ) from the AIRSAR images

$$H_{sT} = \beta^{-2} \int_{\lambda_{c0}}^{\lambda_{cn}} (\lambda_c)^2 d\lambda_c \quad (3)$$

where  $\beta$  is the value of  $\left(c \frac{R}{V}\right)^{-1}$  and  $H_{sT}$  is the significant wave height simulated from AIRSAR images. The introduced method (azimuthal cut off) is designed for homogeneous wave fields as waves can be found over the open ocean under deep water condition with homogeneous bathymetry as can be seen in Figure 1. A linear wave transform model can be used to solve the problem of homogeneous wave fields by simulating the physical wave parameters nearshore.

## 2.5 Wave Refraction Graphical Method

The wave refraction model over the AIRSAR and POLSAR images is formulated on the basis of wave number and wave energy conversation principle, gentle bathymetry slope, steady wave conditions and only depth refractive (Figure 3). According to Herbers et al. (1999) wave refraction equation takes the following form:

$$\frac{\partial}{\partial x} (H_s^2 c_g \cos \phi) + \frac{\partial}{\partial y} (H_s^2 c_g \sin \phi) = 0 \quad (4)$$

where the coordinates and the wave angle  $\phi$  are orientated according to the notation of Figure (3). Equation 4 is a first order Partial Differential Equation (PDEs) in the wave direction  $\phi(x, y)$  and significant wave height  $H_s^2(x, y)$  variables; the group velocity  $c_g$  is a known function of the wave period  $T$  and the known local depth  $h(x, y)$ . Following, Herbers et al (1999), the notation of Figure 3, the explicit finite difference scheme, centred in  $x$ , proposed for the solution of equation 4 takes the form:

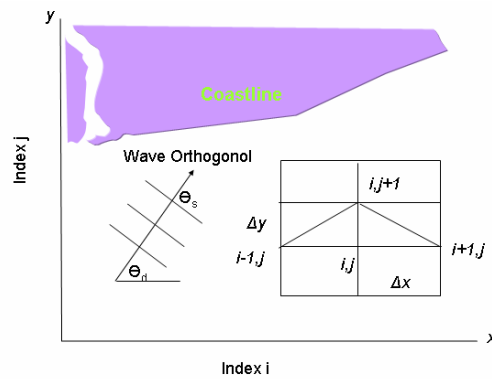


**Figure 3. Method for wave refraction diagram**

(1) Wave direction equation : solved for  $\phi_{ij+1}$

$$\phi_{ij+1} = \arccos \left[ \left( \frac{\Delta y_j}{2} \left( \frac{\sin \phi_{i+1j}}{c_{i+1j}} - \frac{\sin \phi_{ij}}{c_{ij}} \right) \Delta x^{-1} + \left( \frac{\sin \phi_{ij}}{c_{ij}} - \frac{\sin \phi_{i-1j}}{c_{i-1j}} \right) \Delta x^{-1} \right) + \frac{\cos \phi_{ij}}{c_{ij}} \right] \cdot c_{ij+1} \quad (5)$$

(2) Significant wave height equation: solved for  $H_{s_{ij+1}}$

$$H_{s_{ij+1}}^2 = \frac{1}{c_{g_{ij+1}} \sin \phi_{ij+1}} \left[ \frac{(H_{s_{ij}}^2 c_g \sin \phi)_{ij} - 0.5 \Delta y_j \left( \frac{(H_{s_{ij+1}}^2 c_g \cos \phi)_{i+1j}}{\Delta x_i} - \frac{(H_{s_{ij}}^2 c_g \cos \phi)_{ij}}{\Delta x_i} \right)}{(H_{s_{ij}}^2 c_g \cos \phi)_{ij} - H_{s_{ij}}^2 c_g \cos \phi)_{i-1j}} + \frac{(H_{s_{ij}}^2 c_g \cos \phi)_{ij} - H_{s_{ij}}^2 c_g \cos \phi)_{i-1j}}{\Delta x_i - 1} \right] \quad (6)$$

The boundary conditions completing the model are:

- (i) It is assumed that the parallel depth contours as shown in Figure 3
- (ii) The  $\phi$  and  $H_s$  values are given as initial conditions on the open sea boundary ( $j = 1$ ).
- (iii) The computation is terminated on the coastal boundaries ( $h = 0$ ). The wave breaking criterion is applied in shallow waters. The computed significant wave height  $H_s$  is compared to  $0.78 h_{ij}$ ; if  $H_{s_{ij+1}} > 0.78 h_{ij}$ , then
$$H_{s_{ij+1}} = 0.78 h_{ij} \quad (7)$$

The spectra energy of significant wave height distribution due to wave refraction is then estimated by using the following formula adapted from Komar (1976):

$$E(K, H_{s_{ij}}) = S(k_i, k_i) p(H_{s_{ij}}) \quad (8)$$

where  $S(k_i, k_i)$  is the distribution for the wave number and  $p(H_{s_{ij}})$  is the probability distribution of the significant wave height in the convergence and divergence zone. According to Komar (1976), the refraction index ( $K_r$ ) for a straight coastline with parallel contours can be estimated by using the following equation:

$$K_r = \sqrt{\frac{\cos \theta_d}{\cos \theta_r}} \quad (9)$$

where  $\theta_d$  and  $\theta_r$  are the deep and shallow waves incidence angles.

## 2.6 Shoreline Change Model based on Volumetric Change of Sediment Transport (Predicted Method)

The shoreline change model is based on the volumetric change of sediment transport. This mathematical model depends on both the available input of the breaker wave height and direction of deepwater wave height. The alongshore transport rate,  $Q$  (such as cubic

meters per month), is the volumetric rate of the movement of the sand parallel to the shoreline. The calculation of the alongshore transport was based on the assumption that alongshore transport rate,  $Q$ , is only dependent on the alongshore component of the wave energy flux at the breaking point. The shoreline change governing equation used in this study may be expressed as (Komar, 1976)

$$\frac{\partial y}{\partial t} + D^{-1} \frac{\partial Q}{\partial x} = 0 \quad (10)$$

where  $y$  is the shoreline position (m),  $x$  is the alongshore coordinate (m),  $t$  is the time (year),  $D$  is the depth of closure (m), and  $Q$  is the alongshore sand transport rate. In order to solve equation (10) the expressions for the quantity  $D$  must be formulated. The following formula given by Hanson (1989) is used, in which the annual depth of closure is assumed to be twice as deep as the maximum annual significant wave height  $H_{mas}$  as follows  $D = 2H_{mas}$ . The empirical relationship for longshore sand transport assumes that sand is transported alongshore by the acting of breaking significant wave height  $H_{bs}$ . The equation used is (Komar, 1976),

$$Q = 1.1\rho g^{3/2} H_{bs}^{5/2} \sin \alpha_b \cos \alpha_b \quad (11)$$

where  $\rho = 1020 \text{ kg/m}^3$  for the sea water,  $g$  is  $9.8 \text{ m/s}^2$  and  $\alpha_b$  is the breaking wave angle. The significant wave height is determined by using quasi-linear model and the breaking wave  $H_{bs}$  could be obtained by Komar, (1976) as follows

$$H_{bs} = 0.39g^{1/5} (TH_{sT}^2)^{2/5} \quad (12)$$

where,  $T$  is significant wave period, The estimation of AIRSAR/POLSAR breaking significant wave height can be done by replacing the value of AIRSAR significant wave height  $H_{sT}$  into equation 12.

### 2.6.2 Shoreline Change observed from Aerial Photography and AIRSAR and POLSAR data (Observed Method)

The data used to extract shoreline change were a topographic map, aerial photographs data, POLSAR data and AIRSAR data. The topographic map was for 1959 with 1:25,000 scale (Table 1). The vegetation lines in the topographic map, aerial photographs, AIRSAR and POLSAR images were digitized into vector layers. The remote sensing vectors were overlaid with the vectors of the topographic maps. The distance difference ( $\Delta x$ ) was measured. Thus the coastline changes rates could be estimated by  $\Delta x / \Delta t$  where  $\Delta t$  is the time difference. The mathematical model of shoreline change was used to identify the erosion and sedimentation areas. Shoreline change was modeled from ship observation, in situ wave measurements, and remotely sensed data (aerial photographs, AIRSAR and POLSAR images). This model could be used to investigate the places which were exposed to much erosion. Finally, the regression model was used to determine the level of correlation with the predicted and observed models (i.e. shoreline change based on wave spectral effects and shoreline change determined from digitizing



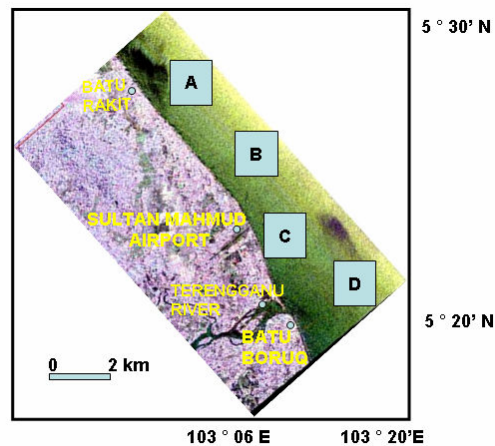
vector layers, respectively). Root mean square error (RMSE) then was used to find the error rates between models.

**Table 1: Remote sensing data for shoreline change**

Type	Data	Date
<b>Topographic map</b>		<b>1959</b>
<b>Optical</b>	<b>Aerial photography</b>	<b>24/8/1980</b>
		<b>26/6/1990</b>
		<b>23/5/1994</b>
<b>SAR data</b>		
<b>Aircraft</b>	<b>AIRSAR</b>	<b>6/12/1996</b>
	<b>POLSAR</b>	<b>19/11/2000</b>

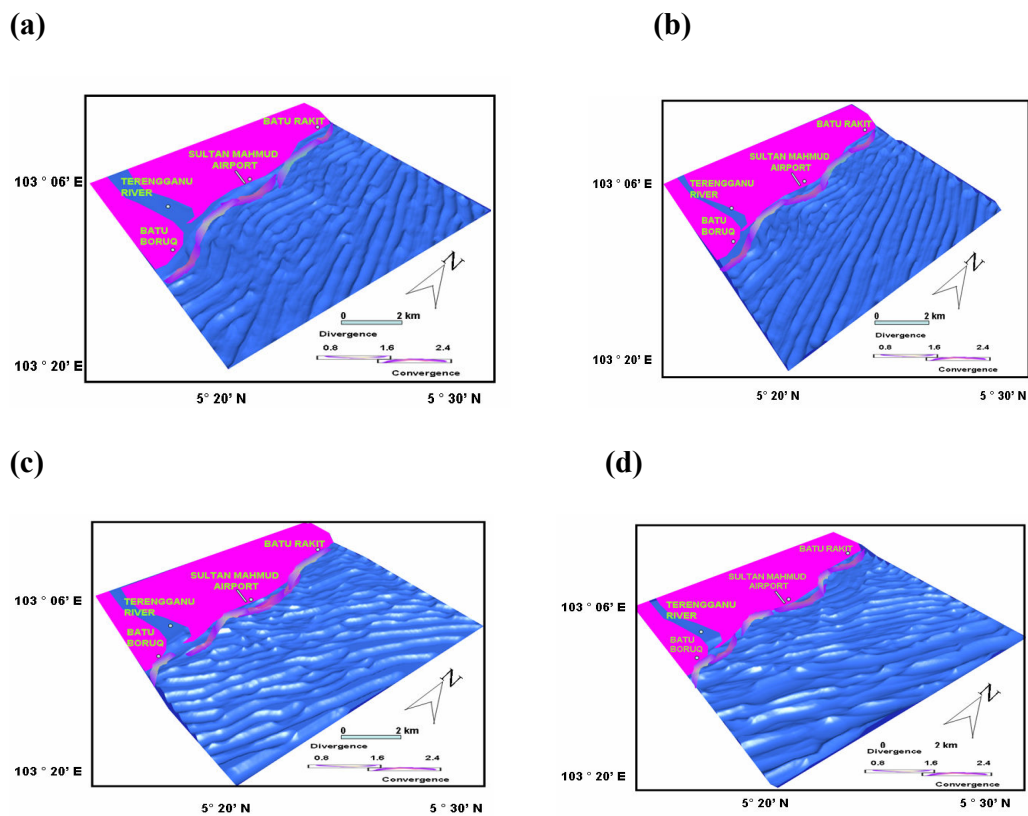
### 3.RESULTS AND DISCUSSION

Figure 4 shows the regions that are used to model the AIRSAR/POLSAR wave spectral information. The wave spectral information have been extracted from the average of four sub-images and each sub-image was 512 by 512 pixels. The average sub-images spectral information were used with the quasi-linear model.



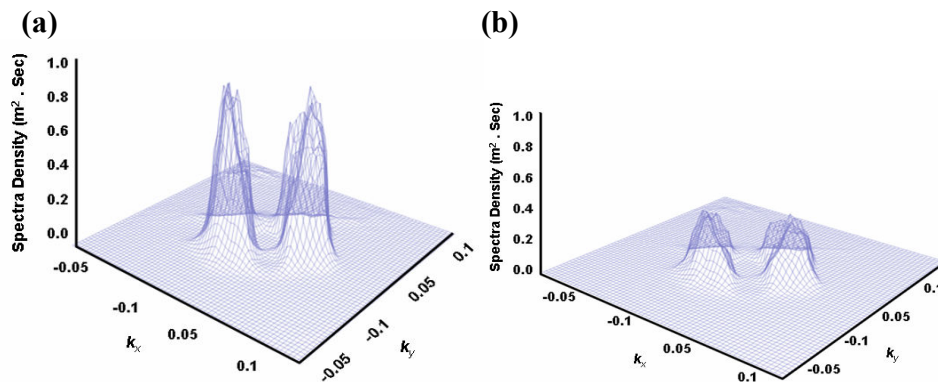
**Figure 4. Location of wave spectra window selections**

Figure 5 shows the wave refraction pattern modeled from the quasi-linear model and in situ wave data. The input quasi-linear wavelength spectra and in situ wavelength spectra were 80 m and 75 m, respectively. Both AIRSAR and POLSAR wave refraction pattern results indicated that the refractive index was 2.60 and 2.54 at the Sultan Mahmed Airport station and the location of Batu Rakit station, respectively, indicating convergence of wave energy (Figure 5). At the Batu Rakit station which is close to the river mouth of Kuala Terengganu, the refractive index values were less than 1.00 indicating divergence of wave energy. In other locations, the refractive index values were close to 0.99, (Figure 5b) indicating no change in the concentration of wave energy at the coastline. Although the refractive index values for the quasi-linear model differed from those of the in situ wave spectra refraction, the same trend of wave energy dispersion and concentration seemed to occur at the coastline. This means that the wave refraction pattern simulated by using the quasi-linear model was similar to the wave refraction simulated from the in situ wave data. The largest refractive index value was observed at the Sultan Mahmed Airport station. This could be attributed to the slight concave shoreline profile which made the incoming north wave energy converge. This result agrees with the findings of Maged (1999) and Maged et al., (2002).



**Figure 5. Wave Refraction Pattern from (a) AIRSAR, (b) in situ measurement 1996, (c) POLSAR and in situ measurement 2000.**

Figure 10 shows the wave refraction spectra energy due to convergence and divergence. The convergence spectrum has sharper peak compared to divergence spectra. The sharp peak of the convergence spectrum is  $0.84 \text{ m}^2 \text{ sec}$  (Figure 6a) while the divergence spectrum peak is less than  $0.4 \text{ m}^2 \text{ sec}$  (Figure 6b). The convergence spectrum peak is located along the azimuth direction. It can be explained that the highest spectra energy propagated close to the azimuth direction is due to the great influence of Doppler frequency shift which is produced by convergence. This result agrees with the study of Vachon et al., (1995).



**Figure 6. Wave refraction spectra (a) convergence and (b) divergence**

In order to evaluate shoreline change utilizing the AIRSAR and POLSAR wave spectra images a comparison has been carried out between rates of shoreline change observed from vector layers of the topographic map of 1959, remotely sensed data (aerial photographs, AIRSAR and POLSAR data) and those predicted from wave spectra effects (quasi-linear and in situ wave data) (Figure 7). The spatial distribution of shoreline change rates revealed remarkable erosion along Sultan Mahmed Airport station with accretion along the Terengganu river and Batu Rakit Station. In the case of the predicted model (quasi-linear model- and in situ wave data) the erosion was greatest at the Sultan Mahmed Airport, namely about  $-2.2 \text{ m/year}$ , and it decreased alongshore until it was reversed to accretion at middle distance between  $6000\text{m}$  and  $8000\text{m}$ . This accretion reached a maximum rate of  $1 \text{ m/year}$ . The accretion rate of  $1 \text{ m/year}$  was also observed between  $12000\text{m}$  and  $16000\text{m}$ . The erosion decreased systematically with alongshore distance which is reduced to  $-0.7 \text{ m/year}$  between  $10000\text{m}$  and  $12000\text{m}$ . The erosion could be attributed to wave energy convergence. Convergence of the wave energy results in the higher and more energetic waves arriving at the shoreline which induces strong longshore sediment transport. The longshore sediment transport was induced by the incoming north wave moving towards the south of Sultan Mahmed Airport and induced sedimentation. The sedimentation could be attributed to wave energy divergence (Figure 9). Thus, accretion could be the result of lower wave energy input from divergence event and it might be due to earlier wave shoaling and sediment transport (Lokman et al., 1995).

**Figure 7: Shoreline rate change from different sorts of data and models.**

The erosion peak modeled from the in situ wave measurements data for the AIRSAR and POLSAR flight times (1996 and 2000) coincided with the one modeled from the quasi-linear and digitizing technique. It is interesting to notice that the shoreline change rate estimated by the observed method (vector layers of the topographic map, historical aerial photography, and AIRSAR/POLSAR images) was approximately similar to the shoreline change pattern modeled from predicted model (in situ wave and quasi-linear model).

Comparison between predicted method (quasi-linear and in situ wave spectra models) and observed method (AIRSAR/POLSAR, aerial photography and topographic map vector layers) using linear regression model indicated a strong square correlation coefficient ( $r^2 = 0.78$ ) (Figure 8). The significant relationship between predicted and observed models was shown by the greater value of statistical F (33.73) than significant F (0.000171) with probability value  $p$  less than 0.05 and accuracy (root mean square error) of  $\pm 0.18$  m/year which is more accurate than that obtained by the observed method (digitizing technique). This error could be raised from the manual digitizing of shoreline. This means that the predicted method of shoreline change from the quasi-linear model can be used as a new approach for study of a large scale shoreline change (Figure 8). The improvement of the quasi-linear model requires more in situ wave measurements and using more AIRSAR/POLSAR data.

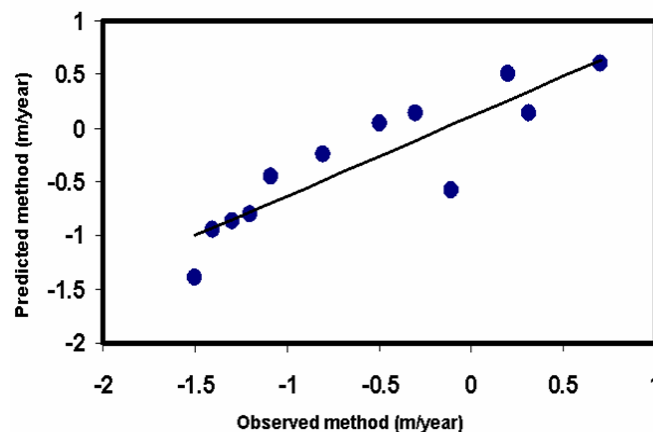


**Figure 8. Regression model of observed and predicted shoreline change [ $y=0.7436 x + 0.113$ ;  $r^2=0.79$ ;  $p<0.05$ ; statistical  $f=33.73$ ; significant  $F=0.000171$  and  $RMSE=\pm 0.18$ m/year]**

In general, the output of this study does not agree with the studies conducted by Stanely (1985), Mazlan et al., (1989) and Maged (2003). This arises from the use of different techniques and different sorts of data. Stanely (1985) did not estimate the sediment volume change rates based on the breaker wave height; instead he used the wave visual observation as the main factor for sediment transport along the shoreline. Mazlan et al. (1989), however, defined the shoreline as the zone of high tide. This definition is not valid because of the fact that the tidal zone is a dynamic area in which the tide changes its cycle between low and high tide. This could not be used as a basic reference for the

shoreline. In addition, Mazlan et al., (1989) have used historical Landsat data for shoreline detection. However, the Landsat image pixel resolution is 30 m which means that the Landsat sensor is unable to capture beach profiles at a width less than the pixel size ( $< 30\text{m}$ ). The present study does not agree with Maged (2003) that the quasi-linear model is not suitable to model shoreline change from SAR data. This could be attributed to the different sort of SAR data used in the two studies. Maged (2003) used an ERS-1 image with highest  $R/V$  value ( $\sim 115\text{s}$ ) compared to AIRSAR/POLSAR images with lowest value of  $R/V$  ( $\sim 32\text{s}$ ). The effect of  $R/V$  in the present study induced a weak nonlinear relationship between AIRSAR/POLSAR image spectra and ocean spectra which could be resolved by utilizing the quasi-linear model. The utilizing of two different periods of AIRSAR and POLSAR data in the present study confirms the previous study of Maged (2001) and improved the accuracy of modeling TOPSAR image spectra effects on shoreline change.

#### **4. CONCLUSIONS**

In this paper we have shown that the ocean wave spectra modeled from AIRSAR and POLSAR  $C_{vv}$ -band can provide valuable and quantitative information on shoreline change modeling with the aid of other remote sensing data of historical aerial photography and topography. It has been demonstrated that the quasi-linear model provides a more accurate shoreline change rate with RMSE value of  $\pm 0.18$  m/year. It can be said that the integration between the quasi-linear model and the continuity model of volume change of sediment transport could be an excellent tool for 2-D shoreline change rate modeling from Airborne SAR data. Furthermore, microwave spectra can be involved in designing micro-small satellite to match with tropical climate circumstances of cloud covers due to its longer wavelength and its polarization properties. This could be used as an early warning system for coastal hazard such as coastal erosion.

#### **Acknowledgements**

We would like to express our appreciation to Universiti Teknologi Malaysia Research Management Center (RMC) for a great cooperation. In fact, RMC is providing excellent advice, plans and management for UTM researchers. We also acknowledge the financial e-science grants have received from the Malaysian Ministry of Science and Technology via its Intensified Research for Priority Areas programme.

#### **References**

- Alpers, W.R., Ross D.B., Rufenach C.L., 1981. On the detectability of ocean surface waves by real and synthetic aperture radar. *Journal of Geophysical Research* 83, 6481-6498.
- Alpers, W., and Bruning C., 1986. On the relative importance of motion-related contributions to SAR imaging mechanism of ocean surface waves. *IEEE Transactions on Geoscience and Remote Sensing* 24, 873-885.

Cornet, Y., Anne C. L, Andre, O., 1993. Significance of wavelength computation using spatial auto-correlation theory on SAR Image of ERS-1. Proceedings of Second ERS-1 Symposium. Hamburg: Germany. pp. 941-944.

Forget, F., Broche, P., Cuq, F., 1995. Principles of swell measurement by SAR with application to ERS-1 observations off the Mauritanian coast. *International Journal of Remote Sensing* 16, 2403-2422.

Hanson, H., 1989. Genesis- a generalised shoreline change numerical model. *Journal of Coastal Research* 5, 1- 27.

Herbers, T. H. C., S. Elgar and R. T. Guza (1999). Directional spreading of waves in the nearshore, *Journal of Geophysical Research*, **104**, 7683-7693.

Hasselmann, K., Hasselmann S., 1991. On the nonlinear mapping of an ocean spectrum and its inversion". *Journal of Geophysical Research*, **96**, 10,713-10,799.

Komar, P.D ., 1976. Beach processes and sedimentation. Prentice-Hall, New Jersey.

Lokman, M.H, Rosnan ,Y., Saas, S., 1995. Beach erosion variability during a north-east monsoon: The Kuala Setiu coastline, Terengganu, Malaysia". *Journal Science Technology Pertanian* 3, 337-348.

Maged, M.M ., 1994. Coastal water circulation off Kuala Terengganu. M.Sc. Thesis, Universiti Pertanian Malaysia.

Maged, M.M., 1999. Prediction of coastal erosion by using radar data. CD of Proceedings of IGARSS' 99. Hamburg, Germany.

Maged, M.M, 2000. Wave spectra studies and shoreline change by remote sensing. Ph. D. Thesis, Universiti Putra Malaysia.

Maged, M.M, 2001. Operational of Canny algorithm on SAR data for modeling shoreline change. *Photogrammetrie Fernerkundung Geoinformation* 2,93-102.

Maged M., 2003. ERS-1 modulation transfer function impact on shoreline change. *International Journal of Applied Earth Observation and Geoinformation*. 4,279-294.

Mazlan, H., Aziz, I., Abdullah, A., 1989. Preliminary evaluation of photogrammetric-remote sensing approach in monitoring shoreline erosion. Proceeding of the 10th Asian Conference on Remote Sensing. November 23-29 1989. Kuala Lumpur. Malaysia . pp. F-5-1-F-5-10.

Populus J., Aristaghes, C., Jonsson, L., Augustin, J.M., Pouliquen, E., 1991. The use of SPOT data for wave analysis. *Remote Sensing of Environment*, **36**, 55-65.

Rosnan , Y., 1987. Geophysical studies in setiu lagoon estuary system. M.Sc. Thesis, Universiti Pertanian Malaysia.

Stanley C. I., 1985. Malaysian national coastal erosion study. Vol II. Kuala Lumpur: UPEN.

Tukey, J.W. 1961. Discussion, emphasizing the connection between analysis of variance and spectrum analysis. *Technometrics*, 3, 191-219.

Vachon P.W., K.E. Harold and J. Scott. 1994. Airborne and Space-borne Synthetic Aperture Radar Observations of ocean waves. *Journal of Atmospheric.-Ocean* 32 ( 10) ; 83-112.

Vachon P.W., A. K. Liu and F.C. Jackson.- 1995. Near-Shore Wave Evolution Observed by Airborne SAR During SWADE. *Journal of Atmospheric.-Ocean* , 2: 363-381.

Vachon, P.W. and J.W.M. Campbell and F.W. Dobson.-1997. Comparison of ERS and Radarsat SARS for Wind and Wave Measurement. *Paper Presented at 3rd ERS Symposium (ESA)* 18-21 March, 1997. Florence, Italy.

Wong, P.P., 1981. Beach change on a monsoon coast, Peninsular Malaysia. *Journal of the Geological Society of Malaysia*, 14, 59-47.

Zebker, H. A., 1992. The TOPSAR interferometric radar topographic mapping instrument. *IEEE Transactions on Geoscience and Remote Sensing*, 30, pp. 933-940.